Low Complexity Discrete Hartley Transform Precoded OFDM System over Frequency-Selective Fading Channel

Xing Ouyang, Jiyu Jin, Guiyue Jin, and Peng Li

Orthogonal frequency-division multiplexing (OFDM) suffers from spectral nulls of frequency-selective fading channels. Linear precoded (LP-) OFDM is an effective method that guarantees symbol detectability by spreading the frequency-domain symbols over the whole spectrum. This paper proposes a computationally efficient and low-cost implementation for discrete Hartley transform (DHT) precoded OFDM systems. Compared to conventional DHT-OFDM systems, at the transmitter, both the DHT and the inverse discrete Fourier transform are replaced by a one-level butterfly structure that involves only one addition per symbol to generate the time-domain DHT-OFDM signal. At the receiver, only the DHT is required to recover the distorted signal with a single-tap equalizer in contrast to both the DHT and the DFT in the conventional DHT-OFDM. Theoretical analysis of DHT-OFDM with linear equalizers is presented and confirmed by numerical simulation. It is shown that the proposed DHT-OFDM system achieves similar performance when compared to other LP-OFDMs but exhibits a lower implementation complexity and peak-to-average power ratio.

Keywords: OFDM, linear precoding, multipath diversity, discrete Hartley transform, DHT, peak-to-average power ratio, PAPR.

Manuscript received Apr. 25. 2014; revised Aug. 7, 2014; accepted Aug. 21, 2014.

Xing Ouyang (christoyx@gmail.com), Jiyu Jin (corresponding author, jiyu.jin@dlpu.edu.cn), Guiyue Jin (guiyue.jin@dlpu.edu.cn), and Peng Li (lipeng@dlpu.edu.cn) are with the School of Information Science & Engineering, Dalian Polytechnic University, Liaoning, China.

I. Introduction

Orthogonal frequency-division multiplexing (OFDM) is an attractive multicarrier transmission technique that has been implemented in wireless and wired broadband communication systems such as LTE, WiMAX, and DVB [1]–[4]. It is spectrally efficient due to the minimized orthogonal subcarrier spacing. By dividing the wideband system spectrum into narrowband subchannels whose response is frequency flat, a single-tap frequency-domain equalizer is more efficient than a time-domain equalizer to compensate frequency-selective fading.

However, conventional OFDM systems are sensitive to the spectral nulls over frequency-selective fading channels because the information symbols transmitted over the subchannels in the vicinity of deep fading may be overwhelmed by noise and can hardly be recovered at the receiver [5]–[6].

Linearly precoded OFDM (LP-OFDM) systems are studied in the literature as attractive alternatives to mitigate the spectral nulls problem [5]–[17]. The basic idea of LP-OFDM is to spread information symbols into either parts of or the whole of the system band by unitary or trigonometric transforms before the symbols are multiplexed by the inverse discrete Fourier transform (IDFT). Therefore, in spite of the spectral nulls, symbols can still be extracted at the receiver.

In [6], it was proved that the maximum achievable multipath diversity order of LP-OFDM equals the number of available channel paths, even with a linear equalizer. In [7]–[8], Debbah and others proposed an isometric random precoded OFDM scheme in which symbols are spread by isometric matrices. The complex field coding was presented to precode the

symbols by truncated matrices [9]. In [7]–[9], the precoding matrices are restricted to being of full column rank; consequently, data rate loss occurs. Linear constellation precoding (LCP) was proposed for OFDM in [10]–[11] without the loss of data rate. To relieve decoding complexity, an optimal grouped LCP in terms of the maximum available multipath diversity was also presented in [10]. However, the complexity of these schemes is still unsatisfactory due to the precoding and decoding processes and symbol detection algorithms.

The LP-OFDM systems based on linear transforms, for which fast calculation algorithms are devised, are attractive for their simplicity and satisfactory performance. For example, the discrete cosine transform (DCT) and Walsh–Hadamard transform (WHT) precoded OFDM were investigated in [12]–[15]. It was shown that the LP-OFDM systems can achieve attractive performance improvement in the frequency-selective fading channels with a linear minimum mean square error (MMSE) equalizer. To further simplify the complexity of LP-OFDM, several works have focused on how to unite the precoding and the multiplexing; that is, making the IDFT processes into a simpler algorithm. For example, the fast algorithms for calculating cascaded WHTs and DFTs are studied in [16]–[19], in which WHTs and DFTs are calculated jointly at a lower complexity than when calculating WHTs and DFTs separately. In [20]–[21], the fast algorithm was applied to the WHT-OFDM system, termed as T-transform, to implement the system more efficiently. In addition, it was shown that the peak-to-average power ratio (PAPR) of the WHT-OFDM signal is improved. In addition, the DHT precoded OFDM (DHT-OFDH) was proposed for its superior PAPR performance [22]–[24]. In [25], we present a simple algorithm to calculate the DHT and IDFT jointly with only one addition operation per symbol.

In this paper, we introduce a more computationally efficient and lower-cost DHT-OFDM scheme than other LP-OFDMs to counteract the spectral nulls problem based on our previous work. In the proposed scheme, the transmitter generates the time-domain DHT-OFDM signal by a simple one-level butterfly structure that involves only one addition operation per symbol. In the receiver, the DFT that is required in other LP-OFDMs and in the conventional DHT-OFDM is avoided, and the frequency-selective fading channel can be compensated by a single-tap equalizer with only a DHT module. Thus, both the computational complexity and system design of the proposed transceiver are simpler and more efficient than that of other LP-OFDMs. Moreover, in this paper, the theoretical BER performance of the proposed DHT-OFDM with both zero-forcing (ZF) and MMSE equalizers is analyzed and confirmed by simulations. It is shown that the proposed scheme has the same ability to mitigate spectral nulls as other LP-OFDM schemes but features much lower PAPR and complexity.

The rest of this paper is organized as follows. The system models of the conventional OFDM and DHT-OFDM are illustrated in Section II. The low-complexity transceiver design for a DHT-OFDM is introduced in Section III. The theoretical performance of the DHT-OFDM is analyzed in Section IV, and a discussion is provided in Section V. In Section VI, simulation is performed to confirm our analysis and the ability of the proposed scheme to counteract the spectral null problem. Finally, Section VII concludes this paper.

II. System Models of DHT-OFDM

1. Conventional OFDM

In Fig. 1, the system diagram of a conventional OFDM system (excluding the dashed frame) is illustrated. For any given number of symbols, we can group the symbols in the frequency domain as $\mathbf{x} = [x(0), x(1), \ldots, x(N-1)]^{\mathrm{T}}$, where the superscript $(\cdot)^{\mathrm{T}}$ denotes the transpose operator and N is the number of subcarriers. The symbols are multiplexed by an IDFT, which can be implemented by taking an inverse fast Fourier transform (IFFT), as in

$$\mathbf{s} = W^{\mathrm{H}}\mathbf{x}, \tag{1}$$

where $\mathbf{s}$ is the time-domain signal vector, W is the DFT matrix with its (m, n)th element being $(1/\sqrt{N})\, e^{-\mathrm{j}2\pi mn/N}$, and $(\cdot)^{\mathrm{H}}$ denotes the Hermitian transpose operator. The time-domain signal is then parallel-to-serial (P/S) converted. To keep the signal from the interference of previously delayed signals and to convert the channel to be circulant, a cyclic prefix (CP), which is the last N_{c} replicas of $\mathbf{s}$, is attached to the beginning of $\mathbf{s}$. The length of CP, N_{c}, is chosen to be larger than the maximum delay spread. The discrete signal is digital-to-analog (D/A) converted for transmission.

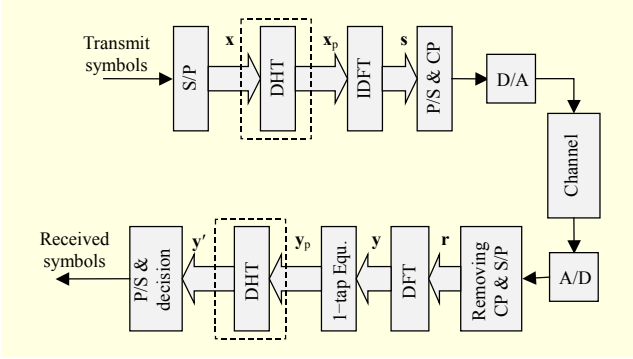

Fig. 1. Conventional OFDM system (excluding the dashed frame) and conventional DHT-OFDM system (including the dashed frame).

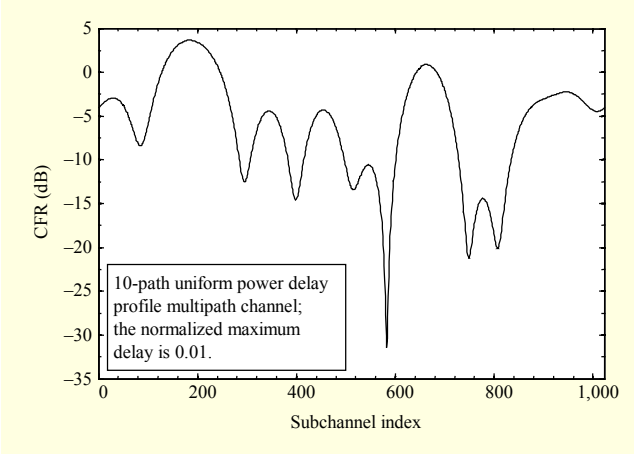

Fig. 2. 10-path uniform power channel in OFDM systems with 1,024 subchannels.

At the receiver, the signal-experiencing multipath channel is received, and CP is discarded directly. The received signal is

$$\mathbf{r} = H\mathbf{s} + \mathbf{n}, \tag{2}$$

where $\mathbf{n}$ is the additive white Gaussian noise (AWGN) and H is the quasi-static channel impulse response (CIR) matrix; that is, the channel is invariant during one OFDM block.

$$H = \begin{pmatrix} h(0) & 0 & \cdots & h(1) \\ h(1) & h(0) & \cdots & h(2) \\ \vdots & \vdots & \ddots & \vdots \\ 0 & 0 & \cdots & h(0) \end{pmatrix}, \tag{3}$$

with $h(l)$, $l = 0, 1, \ldots, L-1$, to be the CIR of the lth channel path. The received signal is transformed by a fast Fourier transform (FFT) to the frequency domain as

$$\mathbf{y} = W\mathbf{r} = WHW^{\mathrm{H}}\mathbf{x} + W\mathbf{n} = \Lambda\mathbf{x} + \mathbf{v}, \tag{4}$$

where $\mathbf{v}$ is the AWGN in the frequency domain and Λ is the channel frequency response (CFR) matrix, which is diagonal with its (k, k)th element, as $H(k)$, representing the channel response on the kth subchannel. The frequency-domain signal is equalized for decision to recover the transmitted information.

In broadband OFDM systems, although each subchannel experiences flat fading, the whole spectrum is still frequency selective. Therefore, some of the subchannels suffer from deep fading. In Fig. 2, the CFR of a 10-path channel with uniform power delay profile (PDP) is sketched. There are deep notches over the spectrum. This shows that symbols on the subchannels in the vicinity of nulls cannot be recovered correctly.

2. Conventional DHT-OFDM

The Hartley transform is a Fourier-related transform [26], and its discrete form was first introduced by Bracewell in 1983 [27]. The obvious differences compared with a DFT are that the forward DHT is identical to the inverse DHT and is real-valued. Various fast algorithms, termed as Fast Hartley Transforms, have been proposed to simplify the implementation complexity, which is said to be similar to that of an FFT.

The block diagram of the conventional DHT-OFDM is illustrated in Fig. 1 (including the dashed frame). In contrast to conventional OFDMs, before the multiplexing of frequency-domain symbols by an IDFT, the symbols are transformed by a DHT into the Hartley domain at the transmitter, and the precoded signal is

$$\mathbf{x}_{\mathrm{p}} = F\mathbf{x}, \tag{5}$$

where F denotes the DHT matrix with its (m, n)th element to be $\mathrm{cas}\,(2\pi mn/N)/\sqrt{N} = [\cos(2\pi mn/N) + \sin(2\pi mn/N)]/\sqrt{N}$. The precoded signal then undergoes the same signal processing procedures as the conventional OFDM. At the receiver, the received signal is transformed to the frequency domain as

$$\mathbf{y} = W\mathbf{r} = WHW^{\mathrm{H}}F\mathbf{x} + W\mathbf{n} = \Lambda F\mathbf{x} + \mathbf{v}, \tag{6}$$

where $\mathbf{v}$ is the frequency-domain noise, and the equalized signal is

$$\mathbf{y}_{\mathrm{p}} = G\mathbf{y} = G\Lambda F\mathbf{x} + G\mathbf{v}, \tag{7}$$

where G is a diagonal weighting matrix based on equalization criteria. The equalized signal is transformed by a DHT for decision.

In the DHT-OFDM, as well as the other LP-OFDM systems, ZF is unfavorable since the noise within the spectral nulls will be amplified and imposed on all symbols after a DHT, resulting in serious performance degradation. The MMSE is a linear equalizer that has better performance due to its capability to suppress noise effectively. The detailed analyses on their performance will be provided in Sections IV and V.

III. Low-Complexity DHT-OFDM

In this section, we propose a computationally efficient and low-cost implementation for the DHT-OFDM illustrated in Fig. 3. At the transmitter, the DHT-OFDM signal is generated by a one-level butterfly structure that realizes a DHT and an IDFT jointly, and the receiver scheme requires only a DHT without a DFT to recover the distorted signal with simplified system design.

In a DHT-OFDM system, the baseband time-domain signal, $\mathbf{s}$, is virtually obtained by substituting (5) into (1), which gives

$$\mathbf{s} = W^{\mathrm{H}}\mathbf{x}_{\mathrm{p}} = W^{\mathrm{H}}F\mathbf{x}. \tag{8}$$

The DHT and DFT matrices can be expressed as $F = C + S$ and

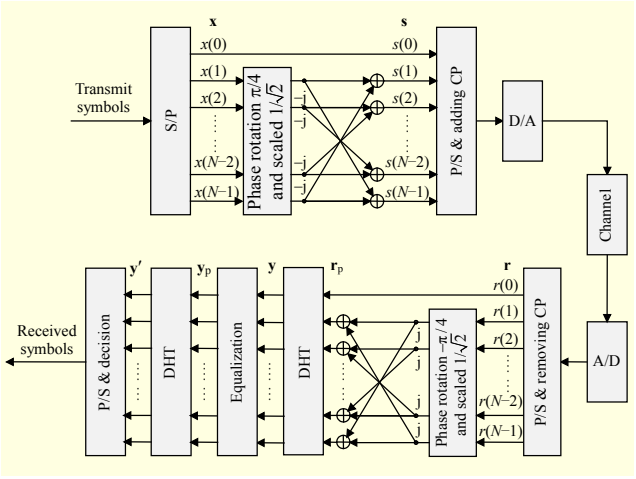

Fig. 3. Proposed low-complexity DHT-OFDM system.

$W = C - \mathrm{j}\,S$, respectively, where the (m, n)th elements of C and S are, respectively,

$$\frac{1}{\sqrt{N}}\cos\left(\frac{2\pi}{N}mn\right) \quad \text{and} \quad \frac{1}{\sqrt{N}}\sin\left(\frac{2\pi}{N}mn\right). \tag{9}$$

It can be readily deduced that the DHT matrix can be expressed in terms of a DFT matrix as

$$\begin{aligned} F &= \frac{1}{2}\left[W + W^{\mathrm{H}} + \mathrm{j}\left(W - W^{\mathrm{H}}\right)\right] \\ &= \frac{1}{2}\left[(1+\mathrm{j})W + (1-\mathrm{j})W^{\mathrm{H}}\right]. \end{aligned} \tag{10}$$

By exploiting the properties of DFT; that is, $W^{\mathrm{H}}W = I$ with I being the unitary matrix, and $WW = J$, where

$$J = \begin{pmatrix} 1 & 0 & 0 & 0 \\ 0 & 0 & 0 & 1 \\ 0 & 0 & \iddots & 0 \\ 0 & 1 & 0 & 0 \end{pmatrix}_{N\times N} \tag{11}$$

is a $N \times N$ flip matrix, and substituting (10) into (8), it can be derived that

$$\begin{aligned} \mathbf{s} &= W^{\mathrm{H}}F\mathbf{x} \\ &= \frac{\sqrt{2}}{2}e^{\mathrm{j}\frac{\pi}{4}}\left(I - \mathrm{j}\cdot J\right)\mathbf{x} \\ &= P\mathbf{x}. \end{aligned} \tag{12}$$

Obviously, instead of the cascaded DHT and DFT operations, the time-domain signal can be generated by combining $\mathbf{x}$ and $\mathbf{x}$ flipped by J with a phase difference of $\pi/2$. Substantially, the nth time sample can be obtained by adding the nth frequency symbol with the symbols on the $(N-n)$th, $n = 1, 2, \ldots, N-1$, subchannel, as in

$$s(n) = \frac{\sqrt{2}}{2}e^{\mathrm{j}\frac{\pi}{4}}\left[x(n) - \mathrm{j}\cdot x(N-n)\right], \tag{13}$$

where $s(n)$ and $x(n)$ are the nth entry of $\mathbf{s}$ and $\mathbf{x}$, respectively.

The proposed transmitter of the DHT-OFDM based on the one-level butterfly structure is illustrated in Fig. 3. The symbols are firstly scaled and phase shifted, and then $\mathbf{x}$ is obtained using a one-level butterfly-like structure. Thereby, the transmitter is simplified to generate the baseband time-domain signal without multiplication except for a scalar and a phase rotation of $\pi/4$.

In this paper, a receiver scheme with only a DHT is proposed, as shown in Fig. 3. Instead of a DFT, the received signal after A/D and S/P conversion is transformed by $P^{\mathrm{H}} = (W^{\mathrm{H}}F)^{\mathrm{H}}$ as

$$\begin{aligned} \mathbf{r}_{\mathrm{p}} &= P^{\mathrm{H}}\mathbf{r} = \frac{\sqrt{2}}{2}e^{-\mathrm{j}\frac{\pi}{4}}\left(I + \mathrm{j}\cdot J\right)\mathbf{r} = \left(W^{\mathrm{H}}F\right)^{\mathrm{H}}\mathbf{r} \\ &= FWHW^{\mathrm{H}}F\mathbf{x} + FW\mathbf{n} \\ &= F\Lambda F\mathbf{x} + F\mathbf{v}. \end{aligned} \tag{14}$$

The third equation in (14) can be readily deduced from (12). The received signal, $\mathbf{r}_{\mathrm{p}}$, is obtained by the one-level butterfly structure by weighting the received signal with P^{H}. Therefore, the frequency-domain signal can be obtained by a DHT, since a DHT is unitary; that is, $F^{\mathrm{H}}F = I$, as

$$\mathbf{y} = F\mathbf{r}_{\mathrm{p}} = \Lambda F\mathbf{x} + \mathbf{v}. \tag{15}$$

At the receiver, the frequency signal can be compensated by a single-tap equalizer based on ZF or MMSE. For the ZF equalizer, the weighting matrix G is Λ^{-1}. The corresponding equalized signal in (7) can be given by

$$\mathbf{y}_{\mathrm{ZF}} = \mathbf{x}_{\mathrm{p}} + \Lambda^{-1}\mathbf{v}, \tag{16}$$

and the signal transformed to the Hartley domain by a DHT is

$$\begin{aligned} \mathbf{y}'_{\mathrm{ZF}} &= F\mathbf{y}_{\mathrm{ZF}} = \mathbf{x} + F\Lambda^{-1}\mathbf{v} \\ &= \mathbf{x} + \mathbf{z}_{\mathrm{ZF}}, \end{aligned} \tag{17}$$

where $\mathbf{z}_{\mathrm{ZF}}$ is the noise vector after ZF equalization. It can be seen that the channel can be completely compensated, but $\mathbf{x}$ will be severely corrupted by the amplified noise. The MMSE equalizer is an attractive equalizer that can suppress the noise at spectrum nulls, and the equalized signal in the Hartley domain is

$$\begin{aligned} \mathbf{y}'_{\mathrm{MMSE}} &= FG_{\mathrm{MMSE}}\,\mathbf{y} \\ &= F\left(\Lambda^{\mathrm{H}}\Lambda + \frac{1}{\lambda}I\right)^{-1}\Lambda^{\mathrm{H}}\left(\Lambda F\mathbf{x} + \mathbf{v}\right) \\ &= F\left(D + \frac{1}{\lambda}I\right)^{-1}DF\mathbf{x} + F\left(D + \frac{1}{\lambda}I\right)^{-1}\Lambda^{\mathrm{H}}\mathbf{v}, \end{aligned} \tag{18}$$

where G_{MMSE} is the coefficient matrix based on MMSE, λ is the signal-to-noise ratio (SNR), and $D = \Lambda^{\mathrm{H}}\Lambda$ is an N by N real diagonal matrix with its (k, k)th element represented by $|H(k)|^2$.

IV. Performance Analysis

In this section, the BER performance of the conventional OFDM and DHT-OFDM based on both ZF and MMSE equalizers is analytically studied to provide insight into the performance improvement of the DHT-OFDM. Quadrature phase-shift keying (QPSK) is considered in this section for analyzing the performance, but the principle can be extended to other modulation formats.

The BER in terms of the SNR in the AWGN channel for QPSK is

$$P_{\mathrm{QPSK}}(\lambda) = Q\left(\sqrt{\lambda}\right), \tag{19}$$

where $Q(x)$ is defined as

$$Q(x) = \frac{1}{\sqrt{2\pi}} \int_{x}^{+\infty} e^{-\frac{t^2}{2}} \mathrm{d}t. \tag{20}$$

In both the AWGN and the frequency-flat fading channels, the DHT-OFDM obtains the same performance as the conventional OFDM system since there is no notch over the spectrum; thus, it provides no frequency diversity. One of the advantages of DHT-OFDM is that it is more robust to frequency-selective fading channels by averaging the deep fading over the whole spectrum, and its performance largely depends on the criteria of equalization.

1. BER Performance of Conventional OFDM System

For the conventional OFDM system, if the ZF equalizer is used, then the equalized signal on the kth subchannel is given by

$$y'_{\mathrm{ZF}}(k) = x(k) + H^{-1}(k)v(k), \tag{21}$$

and, if the MMSE equalizer is used, then the signal is

$$y'_{\mathrm{MMSE}}(k) = \frac{|H(k)|^2}{|H(k)|^2 + \lambda^{-1}} x(k) + \frac{H^*(k)}{|H(k)|^2 + \lambda^{-1}} v(k), \tag{22}$$

where the superscript * denotes the complex conjugate operator. It can be seen that the conventional OFDM system under the frequency-selective fading channel gets the same received SNR, $|H(k)|^2\lambda$, for both ZF and MMSE. Thus, the error probability of the OFDM can be given by

$$\begin{aligned} P_{\mathrm{OFDM}}(\lambda) &= \mathrm{E}\left[\frac{1}{N}\sum_{k=0}^{N-1} P_{\mathrm{QPSK}}\left(|H(k)|^2 \lambda\right)\right] \\ &= \frac{1}{N}\sum_{k=0}^{N-1} \mathrm{E}\left[P_{\mathrm{QPSK}}\left(|H(k)|^2 \lambda\right)\right] \\ &= \frac{1}{N}\sum_{k=0}^{N-1} \mathrm{E}\left[Q\left(\sqrt{|H(k)|^2 \lambda}\right)\right], \end{aligned} \tag{23}$$

where E[·] is the expectation operation.

2. BER Performance of DHT-OFDM Systems

The analysis on BER performance of DHT-OFDM systems is somewhat complicated since the precoded signal is mutually correlated, and the precoding matrix will affect the distribution of noise on each subchannel after equalization.

A. ZF Equalizer for DHT-OFDM

For the ZF equalizer, a signal can be compensated completely; thus, the equivalent channel gain (ECG) is equal to one, as shown in (17). The noise on the kth subchannel, from (17), is

$$z_{\mathrm{ZF}}(k) = \frac{1}{\sqrt{N}} \sum_{n=0}^{N-1} \mathrm{cas}\left(\frac{2\pi}{N} kn\right) H^{-1}(n) v(n). \tag{24}$$

The noise variance after equalization can be deduced as

$$\varepsilon_{\mathrm{ZF}} = \mathrm{E}\left[\frac{1}{N}\sum_{k=0}^{N-1} z^*_{\mathrm{ZF}}(k) z_{\mathrm{ZF}}(k)\right] = \frac{\sigma_n^2}{N}\sum_{n=0}^{N-1} |H(n)|^{-2}, \tag{25}$$

where σ_n^2 is the power of noise **v**. Since the noise $z_{\mathrm{ZF}}(k)$ is a function of the independent random variables $v(n)$ and $H(n)$, $n = 0, 1, \ldots, N-1$ ($H(n)$ are mutually correlated), the noise power imposed on the kth subchannel can be deduced as

$$\begin{aligned} \sigma^2_{\mathrm{ZF}}(k) &= \mathrm{E}\left[z^*_{\mathrm{ZF}}(k) z_{\mathrm{ZF}}(k)\right] \\ &= \frac{\sigma_n^2}{N}\sum_{n=0}^{N-1} \mathrm{cas}^2\left(\frac{2\pi}{N} kn\right) |H(n)|^{-2}. \end{aligned} \tag{26}$$

Hence, the BER of the DHT-OFDM with ZF equalizer is

$$\begin{aligned} P_{\mathrm{ZF}} &= \mathrm{E}\left[\frac{1}{N}\sum_{k=0}^{N-1} P_{\mathrm{QPSK}}\left(\frac{E_s}{\sigma^2_{\mathrm{ZF}}(k)}\right)\right] \\ &= \frac{1}{N}\sum_{k=0}^{N-1} \mathrm{E}\left[Q\left(\sqrt{\frac{\lambda}{\frac{1}{N}\sum_{n=0}^{N-1} \mathrm{cas}^2\left(\frac{2\pi}{N} kn\right)|H(n)|^{-2}}}\right)\right], \end{aligned} \tag{27}$$

where E_s is the symbol energy, which is a constant for PSK.

B. MMSE Equalizer for DHT-OFDM

For the MMSE, the symbols in the Hartley domain are shown in (18), and the desired kth symbol at the receiver is given by

$$\begin{aligned} x'_{\mathrm{MMSE}}(k) &= \left[\frac{1}{N}\sum_{m=0}^{N-1} \mathrm{cas}^2\left(\frac{2\pi}{N} km\right) \frac{|H(m)|^2}{|H(m)|^2 + \lambda^{-1}}\right] x(k) \\ &= |H'(k)| x(k), \end{aligned} \tag{28}$$

where $|H'(k)|$ is defined as the ECG of the kth frequency-domain symbol for MMSE. The residual inter-carrier interference (ICI) and the noise on the kth symbol are

$$x'_{\mathrm{ICI}}(k)=\frac{1}{N}\sum_{n=0,n\neq k}^{N-1}x(n)\times\left[\sum_{m=0}^{N-1}\mathrm{cas}\left(\frac{2\pi}{N}km\right)\mathrm{cas}\left(\frac{2\pi}{N}mn\right)\frac{|H(m)|^2}{|H(m)|^2+\lambda^{-1}}\right] \quad (29)$$

and

$$z_{\mathrm{MMSE}}(k)=\frac{1}{\sqrt{N}}\sum_{n=0}^{N-1}\mathrm{cas}\left(\frac{2\pi}{N}kn\right)\frac{H^*(n)}{|H(n)|^2+\lambda^{-1}}v(n), \quad (30)$$

respectively. Thus, the noise power on the kth symbol is

$$\sigma^2_{\mathrm{MMSE}}(k)=\mathrm{E}\left[z^*_{\mathrm{MMSE}}(k)z_{\mathrm{MMSE}}(k)\right]=\frac{\sigma_n^2}{N}\sum_{m=0}^{N-1}\mathrm{cas}^2\left(\frac{2\pi}{N}km\right)\frac{|H(m)|^2}{\left(|H(m)|^2+\lambda^{-1}\right)^2}. \quad (31)$$

Compared with ZF, even if there is a deep fading; that is, a small $|H(n)|^2$, the noise power can be effectively suppressed. Moreover, the symbols are no longer ICI free. The kth desired symbol will be interfered by ICI as indicated in (29), and the ICI power is

$$\sigma^2_{\mathrm{ICI}}(k)=\mathrm{E}\left[\left|x'_{\mathrm{ICI}}(k)\right|^2\right]. \quad (32)$$

Since $x(k)$ are mutually independent, (32) can be given as

$$\sigma^2_{\mathrm{ICI}}(k)=\frac{E_s}{N}\sum_{m=0}^{N-1}\mathrm{cas}^2\left(\frac{2\pi}{N}km\right)\left[\frac{|H(m)|^2}{|H(m)|^2+\lambda^{-1}}\right]^2-\frac{E_s}{N^2}\left[\sum_{m=0}^{N-1}\mathrm{cas}^2\left(\frac{2\pi}{N}km\right)\frac{|H(m)|^2}{|H(m)|^2+\lambda^{-1}}\right]^2. \quad (33)$$

The first term in (33) is the power of signal $y'_{\mathrm{MMSE}}(k)$ and the second term is the desired signal power $|H'(k)|^2E_s$, which can be readily deduced from (18) and (28). The ICI can be modeled as Gaussian if N is large, and the interference plus noise can be deduced as

$$\begin{aligned}\sigma^2(k)&=\sigma^2_{\mathrm{ICI}}(k)+\sigma^2_{\mathrm{MMSE}}(k)\\&=\frac{E_s}{N}\sum_{m=0}^{N-1}\mathrm{cas}^2\left(\frac{2\pi}{N}km\right)\left[\frac{|H(m)|^2}{|H(m)|^2+\lambda^{-1}}\right]^2\\&\quad-|H'(k)|^2E_s+\frac{\sigma_n^2}{N}\sum_{m=0}^{N-1}\mathrm{cas}^2\left(\frac{2\pi}{N}km\right)\frac{|H(m)|^2}{\left(|H(m)|^2+\lambda^{-1}\right)^2} \quad (34)\\&=\frac{E_s}{N}\sum_{m=0}^{N-1}\mathrm{cas}^2\left(\frac{2\pi}{N}km\right)\left[\frac{|H(m)|^2}{|H(m)|^2+\lambda^{-1}}\right]-|H'(k)|^2E_s\\&=E_s\left[|H'(k)|-|H'(k)|^2\right],\end{aligned}$$

where $|H'(k)|$ is defined in (28) as the equivalent channel gain of the kth symbol. Therefore, the signal-to-interference-plus-noise ratio (SINR) can be deduced from (28) and (34) as

$$\begin{aligned}\Gamma(k)&=\frac{|H'(k)|}{1-|H'(k)|}\\&=\frac{\left[\frac{1}{N}\sum_{m=0}^{N-1}\mathrm{cas}^2\left(\frac{2\pi}{N}km\right)\frac{|H(m)|^2}{|H(m)|^2+\lambda^{-1}}\right]}{1-\left[\frac{1}{N}\sum_{m=0}^{N-1}\mathrm{cas}^2\left(\frac{2\pi}{N}km\right)\frac{|H(m)|^2}{|H(m)|^2+\lambda^{-1}}\right]}.\end{aligned} \quad (35)$$

By exploiting the equation

$$\frac{1}{N}\sum_{m=0}^{N-1}\mathrm{cas}^2\left(\frac{2\pi}{N}km\right)=1, \quad (36)$$

the SINR in (35) can be further simplified as

$$\Gamma(k)=\frac{\sum_{m=0}^{N-1}\mathrm{cas}^2\left(\frac{2\pi}{N}km\right)\frac{|H(m)|^2}{|H(m)|^2+\lambda^{-1}}}{\sum_{m=0}^{N-1}\mathrm{cas}^2\left(\frac{2\pi}{N}km\right)\frac{\lambda^{-1}}{|H(m)|^2+\lambda^{-1}}}. \quad (37)$$

Therefore, the error probability of the DHT-OFDM with MMSE is

$$P_{\mathrm{MMSE}}=\frac{1}{N}\sum_{k=0}^{N-1}\mathrm{E}\left[Q\left(\sqrt{\Gamma(k)}\right)\right]. \quad (38)$$

To show the resistance of DHT-OFDM against spectral nulls, Fig. 4(a) provides a snapshot observation of CFR of a 10-tap multipath channel at SNR = 20 dB. It is obvious that in the conventional OFDM the symbols in the deep notches can hardly be detected correctly, while the ECG of a DHT-OFDM in the Hartley domain $H'(k)$ is flat over the whole spectrum without notches. Although the ECG in the ZF case is always equal to one, the noise will be amplified significantly by $G(k)$, as shown in Figs. 4(b) and 4(c), and spread over all symbols after the DHT, as shown in Fig. 4(d), with pronounced SNR degradation. The MMSE achieves better performance since the coefficients of the taps at nulls can be efficiently suppressed, as shown in Fig. 4(b). Thus, noise power is effectively limited over all the symbols, as shown in Fig. 4(d).

The cumulative distribution function (CDF) of received SNR after the DHT is illustrated in terms of ECG $|H'(k)|^2$ to noise power $|z(k)|^2$ in Fig. 5. At an SNR of 7 dB, the distributions of the conventional OFDM and DHT-OFDM of MMSE superposed together. For the DHT-OFDM with ZF equalizer, about 5 dB SNR loss is incurred if Prob(SNR > SNR_0) = 0.9. Hence, it can be expected that the DHT-OFDM with MMSE achieves similar performance as the conventional

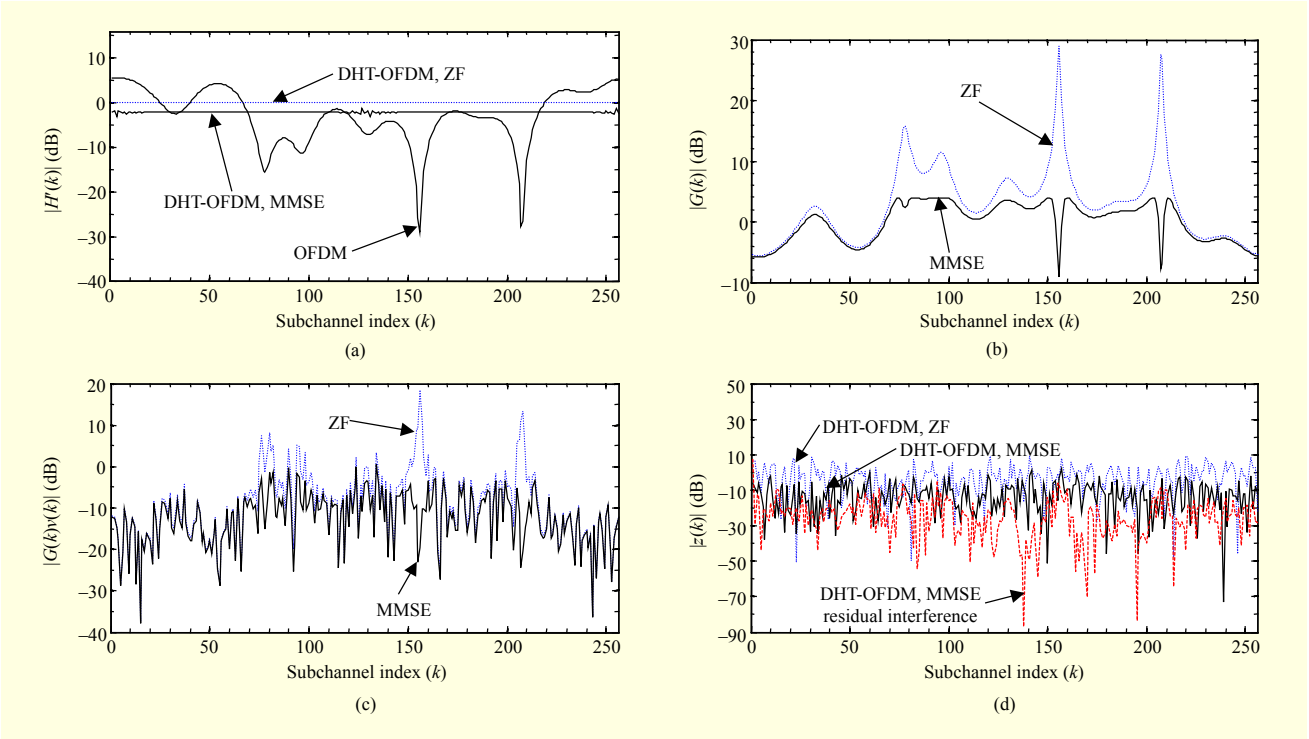

Fig. 4. Snapshots of the conventional OFDM and DHT-OFDM under a frequency-selective fading channel: (a) CFR of the conventional OFDM and equivalent channel gains of the DHT-OFDM after ZF and MMSE equalization in the Hartley domain, (b) equalizers' weights for both ZF and MMSE in the DHT-OFDM, (c) noise $v(k)$ after equalization $G(k)$, and (d) noise being transformed into the Hartley domain $z(k)$ by a DHT.

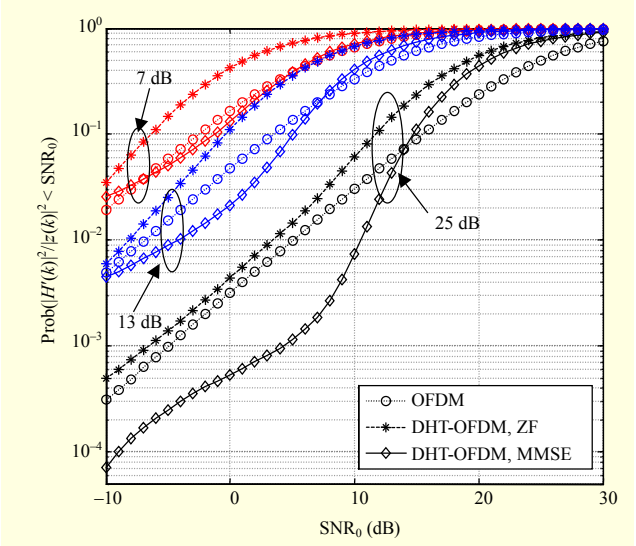

Fig. 5. CDF of received SNR for OFDM and equivalent SNR for DHT-OFDM with ZF and MMSE equalizer with different transmitted SNR.

OFDM at low SNR and that the DHT-OFDM with ZF equalizer exhibits certain performance degradation. As the SNR increases, the DHT-OFDM with MMSE equalizer experiences a significant performance improvement compared to the conventional OFDM; that is, at Prob(SNR > SNR_0) = 10^{-2}, the DHT-OFDM with MMSE sees around a 3 dB to 6 dB improvement for SNR values of 13 dB to 25 dB. Moreover, a 10 dB SNR gain occurs at Prob(SNR > SNR_0) = 10^{-3} at an SNR of 25 dB. Thus, it can be concluded that the performance improvement of the DHT-OFDM with MMSE is more evident at high SNR for its diversity gain.

V. Discussion

In this section, the PAPR of the DHT-OFDM is evaluated and the system complexity is compared with other LP-OFDMs.

1. PAPR of DHT-OFDM

As discussed in (12) and (13) in Section III, the time-domain signal of the DHT-OFDM is the sum of two subcarriers modulated by the mirror symmetrical symbols, rather than the sum of the overall orthogonal subcarriers modulated by different symbols in conventional OFDM systems. Thus, it can be inferred that the peak power of the DHT-OFDM signal can be reduced significantly, as discussed in [22]. The PAPR of the OFDM signal is defined as

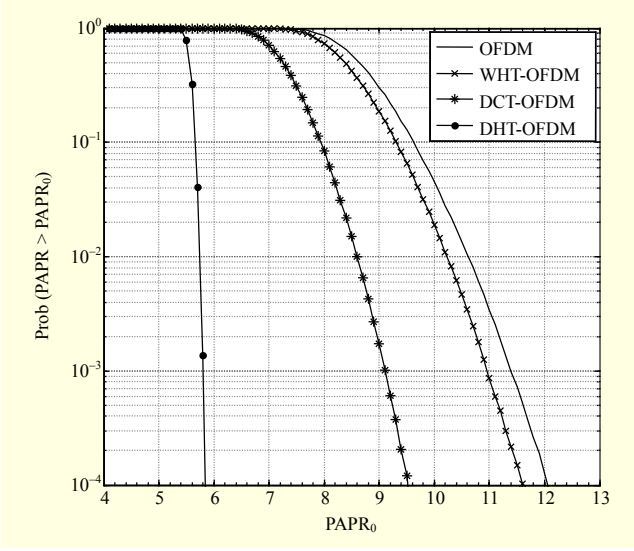

Fig. 6. CCDFs of PAPR for OFDM, DCT-OFDM [20], WHT-OFDM [21], and proposed DHT-OFDM.

$$\mathrm{PAPR} = \frac{\max\left\{\left|s(n)\right|^2\right\}}{\mathrm{E}\left[\left|s(n)\right|\right]}, \tag{39}$$

and the complementary cumulative distribution function (CCDF) of the PAPR is defined as

$$\mathrm{Prob}\left(\mathrm{PAPR} > \mathrm{PAPR}_0\right), \tag{40}$$

which represents the probability of the PAPR of an OFDM signal exceeding a threshold PAPR_0. In Fig. 6, the CCDF of the PAPR is presented for different 16 QAM LP-OFDM systems, and the number of subchannels is $N = 1{,}024$. It can be seen that, both the DCT and the WHT precoded OFDM proposed in [11]–[19] show lower PAPR than the conventional OFDM, with around 2.5 dB and 0.5 dB PAPR improvement at $\mathrm{Prob}(\mathrm{PAPR} > \mathrm{PAPR}_0) = 10^{-4}$. For the DHT-OFDM, the PAPR is reduced further, and the PAPR is reduced by another 3.5 dB and 5.5 dB when compared to the DCT and the WHT precoded OFDM, respectively.

2. Signal Processing and System Design Complexities

In the proposed DHT-OFDM as illustrated in Fig. 3, the DFT is saved by utilizing the properties of both the DHT and the DFT, and two DHTs and two one-level butterfly structures are required. If the input is complex, then the DHT takes $2N\log_2 N$ real multiplications and $3N\log_2 N$ real additions, and the one-level butterfly algorithm takes $2N$ real additions. In addition, the single-tap equalizer at the receiver takes $4N$ real multiplications and $2N$ real additions. Therefore, if the input is complex, then the total number of real multiplications and additions are

$$N_{\mathrm{add.}} = 6(N\log_2 N + N) \tag{41}$$

and

$$N_{\mathrm{multi.}} = 4(N\log_2 N + N), \tag{42}$$

respectively. In the conventional DHT-OFDM as shown in Fig. 1, an FFT, an IFFT, and two DHTs are required. If the input is complex, then the FFT (IFFT) takes $2N\log_2 N$ real multiplications and $4N\log_2 N$ real additions, and the total number of real arithmetic operations is

$$N_{\mathrm{add.}} = 14N\log_2 N + 2N \tag{43}$$

and

$$N_{\mathrm{multi.}} = 8N\log_2 N + 4N, \tag{44}$$

respectively. In Table 1, their complexities are compared, and it can be seen that the complexity of the proposed transceiver is around half of that of the conventional DHT-OFDM.

In the DCT-OFDM, besides the DFT and the IDFT, both the DCT and the IDCT, whose complexity is similar to a DHT, are required. Thus, it can be expected that the complexity of the proposed scheme is about half of that of the DCT-OFDM. In WHT-OFDM, although two T-transforms are applied to perform the WHT and IDFT operations joint at the transmitter [15]–[19], two additional WHTs are required at the receiver, resulting in higher implementation complexity than the proposed DHT-OFDM.

Table 1. Comparison of real arithmetic operations between conventional and proposed DHT-OFDM.

Abbr.	Conventional DHT-OFDM		Proposed DHT-OFDM		Operation reduction (%)	
N	Add.	Multi.	Add.	Multi.	Add.	Multi.
64	5,504	3,328	2,688	1,792	51.2%	46.2%
256	29,184	17,408	13,824	9,216	52.6%	47.1%
1,024	145,408	86,016	67,584	45,056	53.5%	47.6%
4,096	696,320	409,600	319,488	212,992	54.1%	48.0%

VI. Simulation Results

In this section, simulations are performed using MATLAB® to evaluate and confirm the advantages of the proposed DHT-OFDM scheme to provide frequency diversity to improve the performance in frequency-selective channels. The system bandwidth is 10 MHz with 1,024 subchannels, and QPSK and 16 QAM are employed. Both the multipath Rayleigh fading

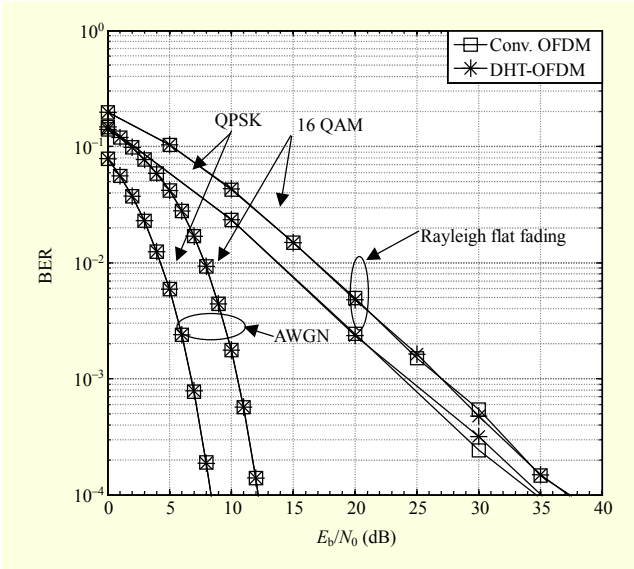

Fig. 7. BER of conventional OFDM and DHT-OFDM under flat-fading channel with QPSK and 16 QAM.

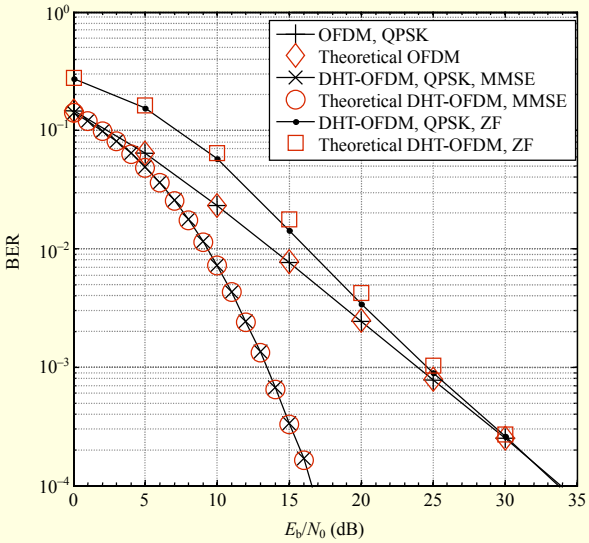

Fig. 8. BER of conventional OFDM and DHT-OFDM under 10-tap multipath fading channel with QPSK.

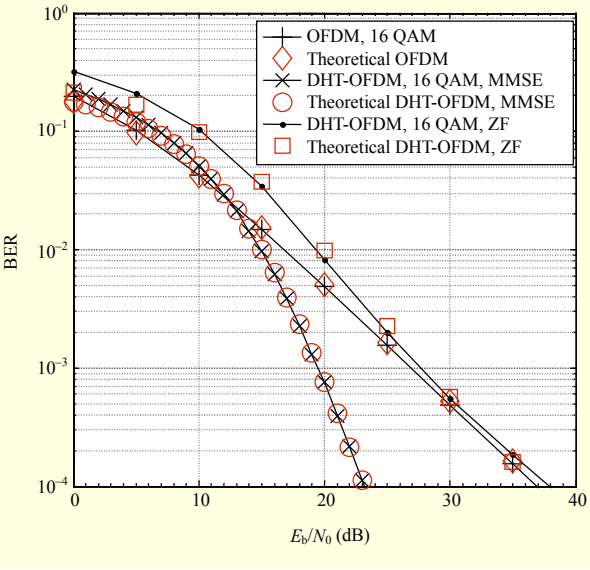

Fig. 9. BER of conventional OFDM and DHT-OFDM under 10-taps multipath fading channel with 16 QAM.

channel and the more realistic ITU channel model B are investigated. The channel response is assumed to be invariant within one OFDM symbol block, and the channel state information is perfectly known at the receiver. The path power is normalized as $\Sigma_l |h(l)|^2 = 1$.

In Fig. 7, simulation is performed under both the AWGN and the flat-fading Rayleigh channels. The conventional OFDM and DHT-OFDM achieve the same BER performance since the DHT-OFDM provides no frequency diversity in the frequency flat-fading channel. In addition, the performances of the DHT-OFDM based on ZF and MMSE are identical since there is no spectral null in a flat-fading channel and the noise will not be amplified.

A frequency-selective channel is considered in Figs. 8–11. In Figs. 8 and 9, a 10-path equal-gain multipath Rayleigh channel with a normalized maximum delay of 0.25 is adopted, and QPSK and 16 QAM are employed, respectively. The MMSE equalizer obtains significant improvement compared with the conventional OFDM and ZF. This is because the frequency nulls are averaged and the noise is effectively suppressed, as analyzed in (31) and (37). Due to the noise enlargement, the DHT-OFDM with ZF is even inferior to conventional OFDM, especially at low SNR. Its performance curve is asymptotically approaching the conventional OFDM as the SNR increases. In addition, the numerical results follow the analytical results as studied in (27) and (38).

In Fig. 10, simulation is performed under ITU channel model B with QPSK, 16 QAM, and 64 QAM formats. It is observed that for 16 QAM and 64 QAM, the conventional OFDM outperforms DHT-OFDM with MMSE at low SNR, and crossover occurs at 12 dB and 20 dB, respectively. A simple explanation is that, at low SNR, the received SNR of all the symbols is averaged below a certain detectable SNR in DHT-OFDM, but for OFDM some of the symbols are still recoverable.

In Fig. 11, simulations are performed for the WHT, DCT, and DHT-OFDM under ITU channel model B. In both the ZF and MMSE schemes of different LP-OFDM, they achieve almost the same BER performance. Thus, it can be inferred that the proposed DHT-OFDM scheme inherits the same ability to exploit the frequency diversity.

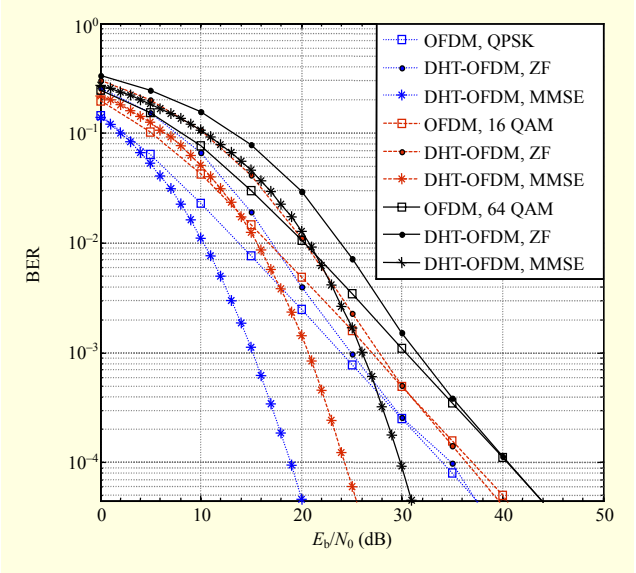

Fig. 10. BER of conventional OFDM and DHT-OFDM under ITU channel model B with QPSK, 16 QAM, and 64 QAM.

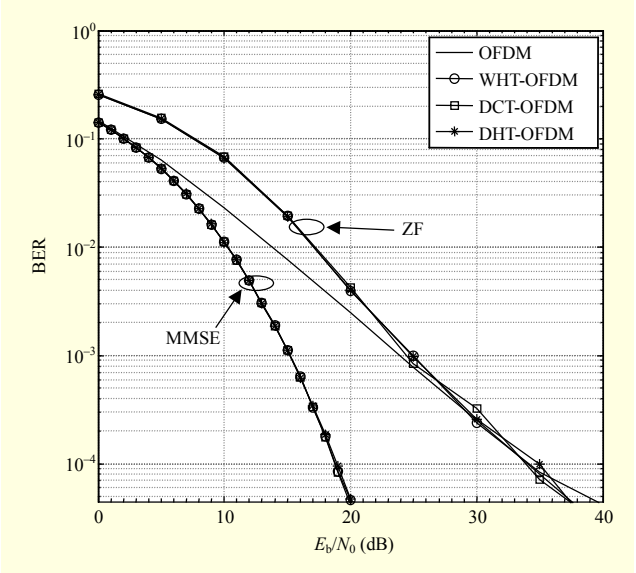

Fig. 11. BER performances of DCT, WHT, and DHT-OFDM under ITU channel model B.

VII. Conclusion

This paper presents a low-complexity DHT precoded OFDM system to mitigate the spectral null problem under frequency-selective fading channels. The precoded signal is obtained using a one-level butterfly structure that requires only additions rather than DHTs and IFFTs, and only a DHT is required at the receiver. Theoretical analysis and simulations confirm that the proposed scheme is robust in frequency-selective channels by spreading symbols into the whole spectrum to exploit the frequency diversity. Compared with other LP-OFDM schemes; for example, WHT and DCT precoded OFDM, the proposed scheme exhibits much lower PAPR and simplified signal processing complexity. Thus, these advantages make the proposed scheme a promising low-cost solution for frequency-selective fading channels.

References

[1] N. Cvijetic, D. Qian, and J. Hu, "100 Gb/s Optical Access Based on Optical Orthogonal Frequency-Division Multiplexing," *IEEE. Commun. Mag.*, vol. 48, no. 7, July 2010, pp. 70–77.

[2] G.L. Stuber et al., "Broadband MIMO-OFDM Wireless Communications," *Proc. IEEE*, vol. 92, Feb. 2004, pp. 271–294.

[3] T. Hwang et al., "OFDM and Its Wireless Applications: A Survey," *IEEE Trans. Veh. Technol.*, vol. 58, no. 4, May 2009, pp. 1673–1694.

[4] J. Zhao and A.D. Ellis, "Advantage of Optical Fast OFDM over OFDM in Residual Frequency Offset Compensation," *IEEE Photon. Technol. Lett.*, vol. 24, 2012, pp. 2284–2287.

[5] Z. Wang and G.B. Giannakis, "Linearly Precoded or Coded OFDM against Wireless Channel Fades?" *Proc. IEEE Workshop Signal Process. Adv. Wireless Commun.*, Taoyuan, Taiwan, Mar. 20–23, 2001, pp. 267–270.

[6] C. Tepedelenlioglu, "Maximum Multipath Diversity with Linear Equalization in Precoded OFDM Systems," *IEEE Trans. Inf. Theory*, vol. 50, no. 1, Jan. 2004, pp. 232–235.

[7] M. Debbah et al., "MMSE Analysis of Certain Large Isometric Random Precoded Systems," *IEEE Trans. Inf. Theory*, vol. 49, no. 5, May 2003, pp. 1293–1311.

[8] M. Debbah, P. Loubaton, and M. de Courville, "Asymptotic Performance of Successive Interference Cancellation in the Context of Linear Precoded OFDM Systems," *IEEE Trans. Commun.*, vol. 52, no. 9, Sept. 2004, pp. 1444–1448.

[9] Z. Wang and G.B. Giannakis, "Complex-Field Coding for OFDM over Fading Wireless Channels," *IEEE Trans. Inf. Theory*, vol. 49, no. 3, Mar. 2003, pp. 707–720.

[10] Z. Liu, Y. Xin, and G.B. Giannakis, "Linear Constellation Precoding for OFDM with Maximum Multipath Diversity and Coding Gains," *IEEE Trans. Commun.*, vol. 51, no. 3, Mar. 2003, pp. 416–427.

[11] Z. Liu, Y. Xin, and G.B. Giannakis, "Space-Time-Frequency Coded OFDM over Frequency-Selective Fading Channels," *IEEE Trans. Signal Process.*, vol. 50, no. 10, Oct. 2002, pp. 2465–2476.

[12] Y.-P. Lin and S.-M. Phoong, "BER Minimized OFDM Systems with Channel Independent Precoders," *IEEE Trans. Signal Process.*, vol. 51, no. 9, Sept. 2003, pp. 2369–2380.

[13] X. Ouyang et al., "Interleaved Multiplexing Optical Fast OFDM without the Interference between Subchannels," *IEEE Photon.*

Technol. Lett., vol. 25, no. 4, Feb. 2013, pp. 378–381.
[14] B. Gaffney and A.D. Fagan, "Walsh-Hadamard Transform Precoded MB-OFDM: An Improved High Data Rate Ultra Wideband System," *Proc. IEEE Int. Symp. PIMRC*, Helsinki, Finland, Sept. 11–14, 2006, pp. 1–5.
[15] X. Ouyang, "Single-Tap Equalization of Fast OFDM Signals under a Generic Linear Channel," *IEEE Commun. Lett.*, vol. 18, no. 8, Aug. 2014, pp. 1319–1322.
[16] M.T. Hamood and S. Boussakta, "Fast Walsh-Hadamard-Fourier Transform Algorithm," *IEEE Trans. Signal Process.*, vol. 59, no. 11, Nov. 2011, pp. 5627–5631.
[17] T. Su and F. Yu, "A Family of Fast Hadamard-Fourier Transform Algorithms," *IEEE Signal Process. Lett.*, vol. 19, no. 9, Sept. 2012, pp. 583–586.
[18] X. Ouyang et al., "Walsh-Hadamard Fourier Transform–Based OFDM with Space-Multipath Diversity," *Proc. IEEE Conf. TENCON*, Xi'an, China, Oct. 22–25, 2013, pp. 1–5.
[19] J. Zhao, "DFT-Based Offset-QAM OFDM for Optical Communications," *Opt. Exp.*, vol. 22, no. 1, 2014, pp. 1114–1126.
[20] M.S. Ahmed et al., "OFDM Based on New Transform with BER Performance Improvement across Multipath Transmission," *Proc. IEEE Int. Conf. Commun.*, Cape Town, South Africa, May 23–27, 2010, pp. 1–5.
[21] M.S. Ahmed, S. Boussakta, and B. Sharif, "OFDM Based on Low Complexity Transform to Increase Multipath Resilience and Reduce PAPR," *IEEE Trans. Signal Process.*, vol. 59, no. 12, Dec. 2011, pp. 5994–6007.
[22] B. Imran and J. Varun, "PAPR Analysis of DHT-Precoded OFDM System for M-QAM," *Int. Conf. Intell. Adv. Syst.*, Kuala Lumpur, Malaysia, June 15–17, 2010, pp. 1–4.
[23] B. Imran and J. Varun, "A New Discrete Hartley Transform Precoding Based Interleaved-OFDMA Uplink System with Reduced PAPR for 4G Cellular Networks," *J. Eng. Sci. Technol.*, vol. 6, no. 6, 2011, pp. 685–694.
[24] X. Ouyang et al., "Low Complexity Discrete Hartley Transform Precoded OFDM for Peak Power Reduction," *Electron. Lett.*, vol. 48, no. 2, Jan. 2012, pp. 90–91.
[25] I. Ali et al., "A DHT Precoded OFDM System with Full Diversity and Low PAPR," *IEEE Int. Symp. Pers. Indoor Mobile Radio Commun.*, Sydney, Australia, Sept. 9–12, 2012, pp. 2383–2388.
[26] R.V.L. Hartley, "A More Symmetrical Fourier Analysis Applied to Transmission Problems," *Proc. IRE*, vol. 30, no. 3, Mar. 1942, pp. 144–150.
[27] R.N. Bracewell, "Discrete Hartley Transform," *J. Opt. Soc. America*, vol. 73, no. 12, 1983, pp. 1832–1835.

Xing Ouyang received his MS degree in information science and engineering from Dalian Polytechnic University, China, in 2013 and is now studying at Tyndall National Institute, University College Cork, Ireland. His main research interests include multicarrier transmission techniques and digital signal processing in both wireless and optical communication systems.

Jiyu Jin received his PhD degree in information and communication engineering from Yeungnam University, Gyeongsan, Rep. of Korea, in 2007. From 2007 to 2008, he was a post-doctoral researcher at the School of Electrical Engineering and Computer Science, Seoul National University, Rep. of Korea. From 2008 to 2009, he was an assistant professor of information and communication engineering at Yeungnam University. He joined the Hilandwe Communication Technology Co., Ltd., Dalian, Liaoning Province, China, as a technical director in 2010. He is currently an associate professor at the School of Information Science and Engineering, Dalian Polytechnic University, China. His research interests include wireless/mobile communication systems and Internet of things.

Guiyue Jin received her PhD degree in computer engineering from Yeungnam University, Gyeongsan, Rep. of Korea, in 2009. She is currently an assistant professor at the School of Information Science and Engineering, Dalian Polytechnic University, China. Her research interests include pervasive computing and wireless communication.

Peng Li received his PhD degree in information and communication engineering from Harbin Institute of Technology, China, in 2009. He is currently an associate professor at the School of Information Science and Engineering, Dalian Polytechnic University, China. His research interests include ad hoc networks and optical communication systems.